Lab3 EECE 5554 Imu & Allan Variance

Introduction:

The IMU unit under study provided multifaceted outputs encompassing angle, magnetic fluctuation, linear acceleration, and angular velocity across the three spatial axes. To ensure a comprehensive analysis, data was collected in two distinct phases. The first phase spanned a 10-minute duration, offering insights into Orientation, Linear Acceleration, Angular Velocity, and Magnetic Fluctuation. This initial dataset was pivotal in establishing foundational understanding and paving the way for a more exhaustive study.

Subsequently, the second phase extended over a remarkable duration of 5 hours. This prolonged data collection was meticulously designed to enable a profound analysis using the Allan Variance method, a tool well-regarded for its ability to analyze the stability of frequency standards.

15 mins data set:

Category	Axis	Standard deviation	mean
Angular	x	0.008825	9.3617e-05
Angular	y	0.00288	4.5299e-05
Angular	z	0.001151	-1.7709e-04
Orientation	x	0.009169	-0.0461
Orientation	y	0.017124	0.2961
Orientation	z	0.003434	-0.4103
Linear	x	0.019294	1.6422
Linear	y	0.069748	7.3521
Linear	z	0.074202	-6.5986
Magnetic	x	0.002732	0.0526
Magnetic	y	0.013230	-0.4405
Magnetic	z	0.007273	0.2742

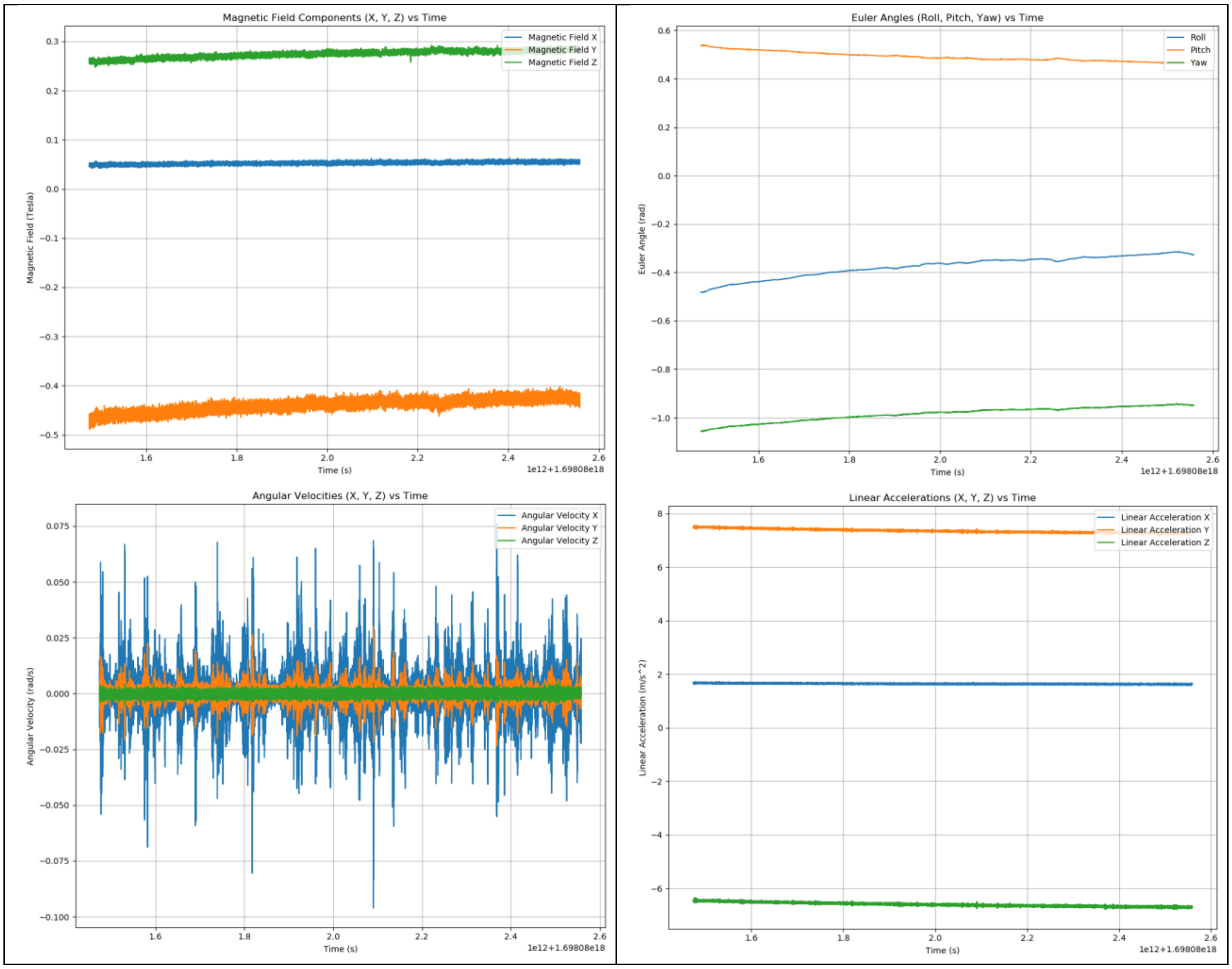
Magnetic Field Components (X, Y, Z) vs Time
Magnetic Field X
Magnetic Field Y
Magnetic Field Z
Magnetic Field (Tesla)
Time (s)
1e12+1.69808e18
Euler Angles (Roll, Pitch, Yaw) vs Time
Roll
Pitch
Yaw
Euler Angle (rad)
Time (s)
1e12+1.69808e18
Angular Velocities (X, Y, Z) vs Time
Angular Velocity X
Angular Velocity Y
Angular Velocity Z
Angular Velocity (rad/s)
Time (s)
1e12+1.69808e18
Linear Accelerations (X, Y, Z) vs Time
Linear Acceleration X
Linear Acceleration Y
Linear Acceleration Z
Linear Acceleration (m/s^2)
Time (s)
1e12+1.69808e18

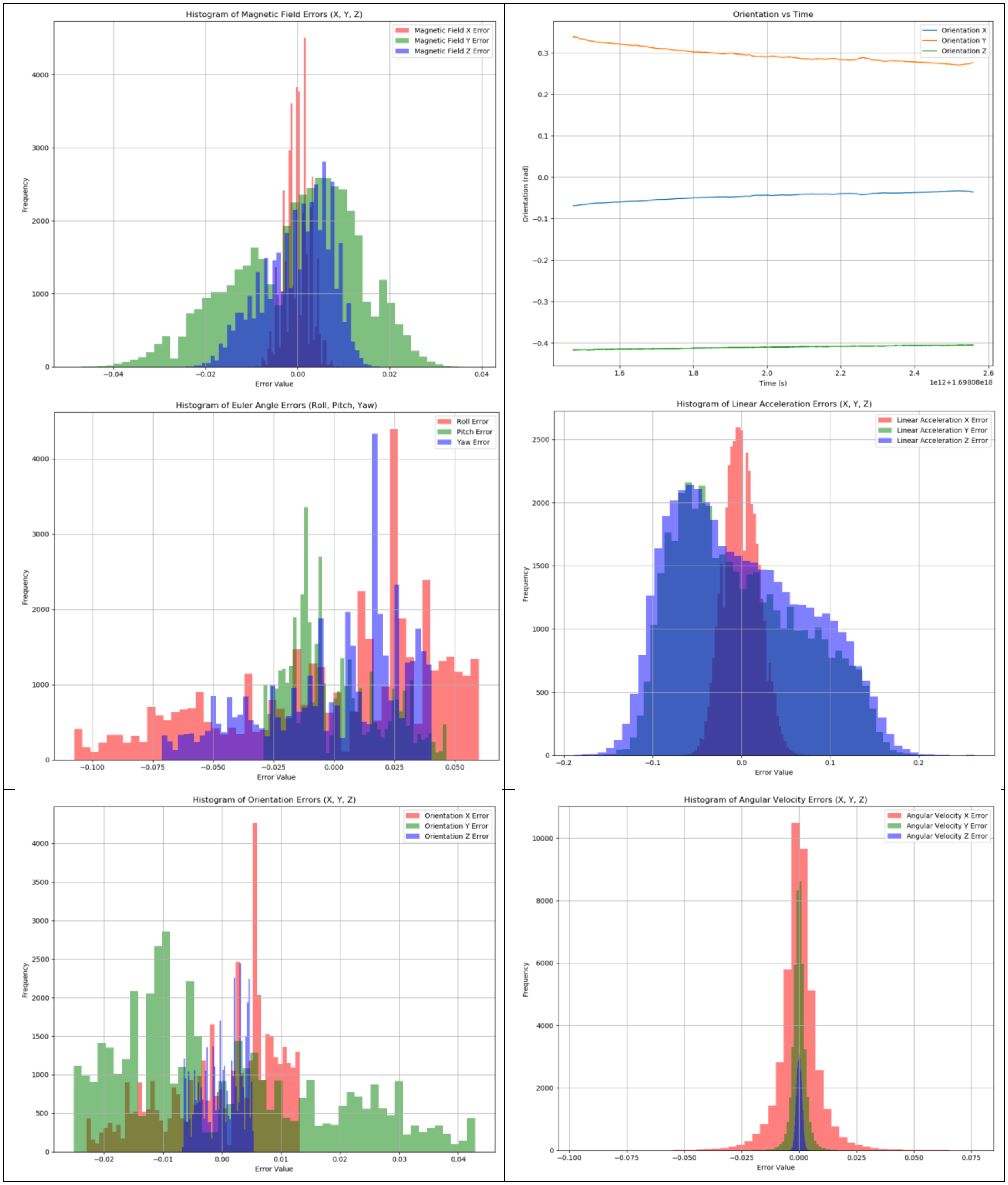

Analysis:

Within a 15-minute dataset span, it's clear that the Angular Velocity, Linear Acceleration, and Magnetic Flux closely follow a normal distribution. However, any noticeable differences from this normal distribution could be because the data is broken down into three axes or due to external interferences, like in the angular velocity and magnetic histograms. For the other two charts, only parts of them seem to follow a normal distribution. This discrepancy might be due to unexpected vibrations from things like nearby trains or the building's structure.

The Orientation and Linear data noticeably deviate from a perfect zero mean, hinting at possible drifts or biases. Meanwhile, the Magnetic data isn't centered around zero, possibly due to external magnetic factors or built-in sensor biases.

When we talk about the conversion process, the data was transformed into quaternions. To ensure the accuracy of this conversion, we used inverse transformation techniques. By comparing the original Euler angles with the newly converted ones and noticing the similar shape in scatter plots for orientation and Euler angles, we're confident that the data's integrity remains intact throughout these processes.

Moreover, the nearly-zero means in the Angular data across all axes suggest a minimal presence of bias or drift, though some sensor noise is evident from the standard deviations.

5 hour Data set:

Sensor	N	K	B
GyroX	1.2310e-05	7.8521e-08	2.0474e-07
GyroY	6.5670e-06	2.0945e-08	5.4612e-08
GyroZ	1.5462e-04	2.4693e-05	6.4384e-05
AccX	6.6897e-04	1.2070e-05	3.1470e-05
AccY	2.6912e-04	6.8586e-08	1.7883e-07
AccZ	6.6026e-04	8.4234e-06	2.1963e-05
QuatX	3.9977e-04	1.8085e-05	4.7155e-05
QuatY	4.8303e-04	1.8505e-05	4.8249e-05
QuatZ	2.7044e-04	1.1842e-05	3.0877e-05
MagX	1.6897e-05	5.3893e-08	1.4052e-07
MagY	3.1079e-05	7.0092e-08	1.8276e-07
MagZ	1.5850e-05	5.0554e-08	1.3181e-07

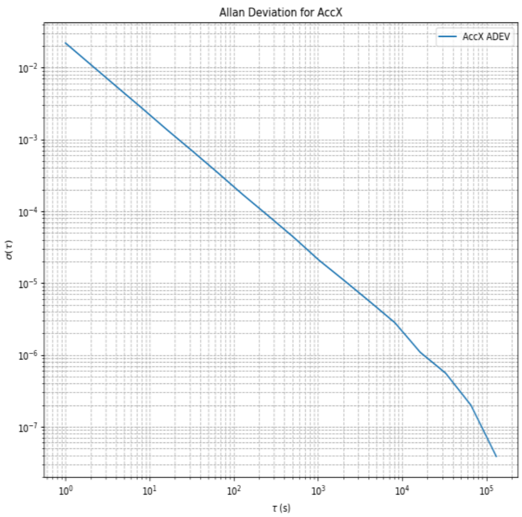
Allan Deviation for AccX
AccX ADEV
σ(τ)
τ (s)

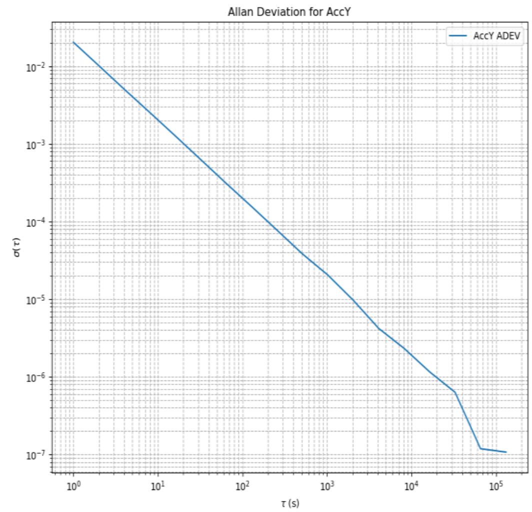
Allan Deviation for AccY
AccY ADEV
σ(τ)
τ (s)

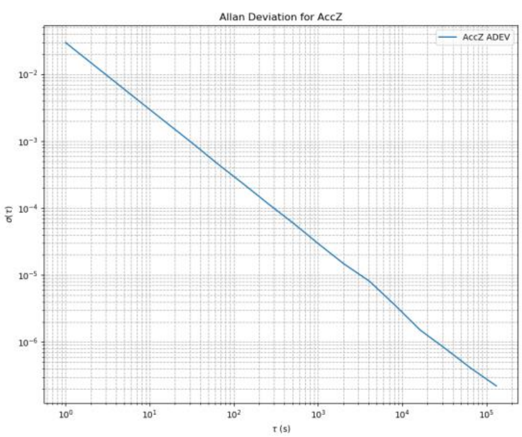
Allan Deviation for AccZ
AccZ ADEV
σ(τ)
τ (s)

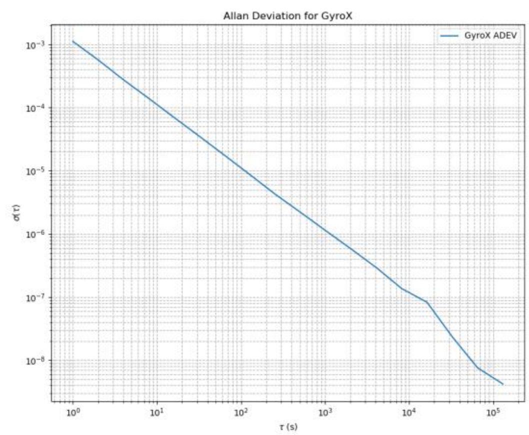
Allan Deviation for GyroX
GyroX ADEV
σ(τ)
τ (s)

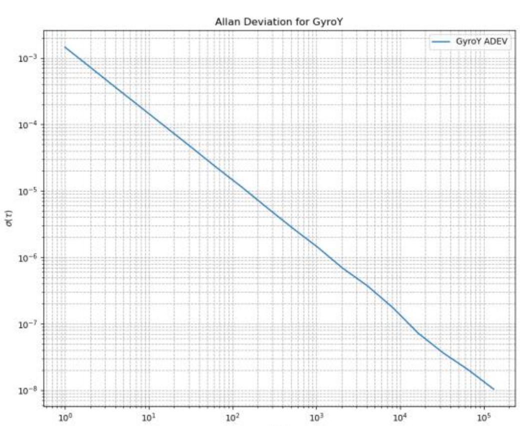
Allan Deviation for GyroY
GyroY ADEV
σ(τ)
τ (s)

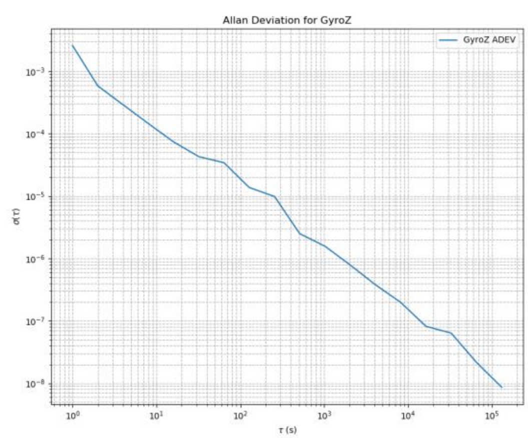
Allan Deviation for GyroZ
GyroZ ADEV
σ(τ)
τ (s)

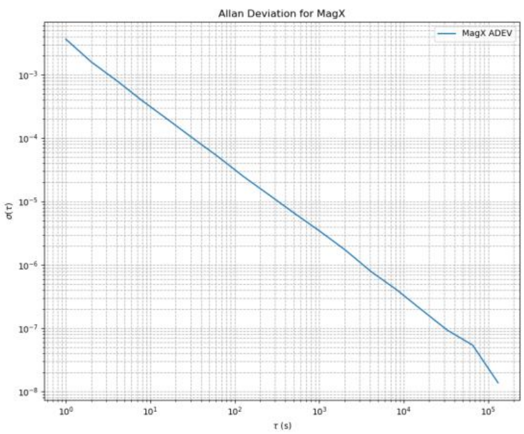
Allan Deviation for MagX
MagX ADEV
σ(τ)
τ (s)

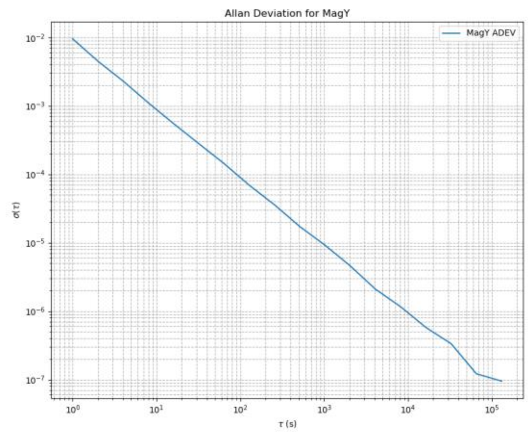
Allan Deviation for MagY
MagY ADEV
σ(τ)
τ (s)

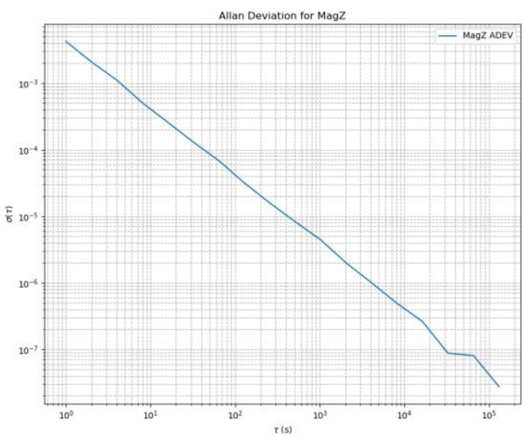
Allan Deviation for MagZ
MagZ ADEV
σ(τ)
τ (s)

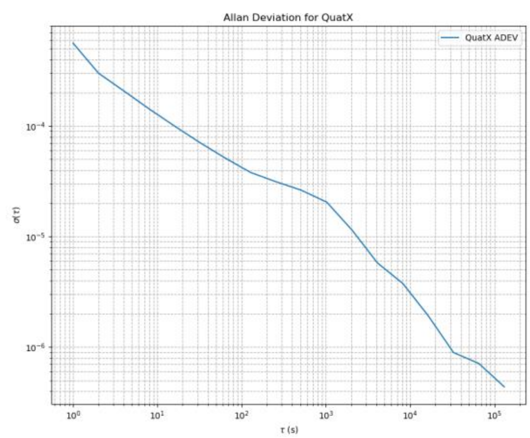
Allan Deviation for QuatX
QuatX ADEV
σ(τ)
τ (s)

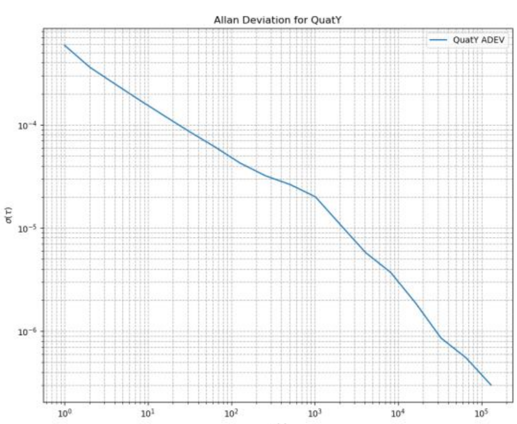
Allan Deviation for QuatY
QuatY ADEV
σ(τ)
τ (s)

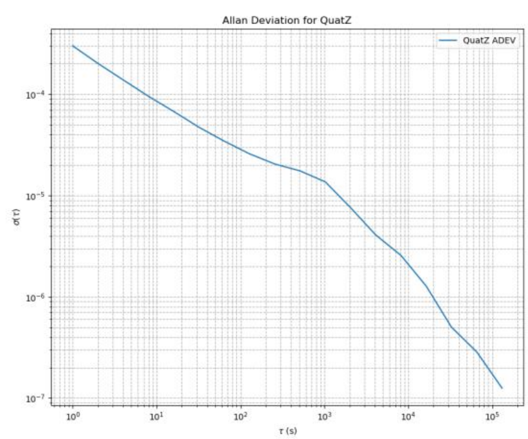
Allan Deviation for QuatZ
QuatZ ADEV
σ(τ)
τ (s)

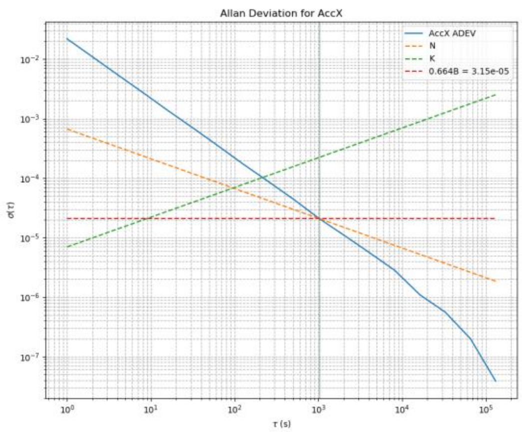
Allan Deviation for AccX
AccX ADEV
N
K
0.664B = 3.15e-05
σ(τ)
τ (s)

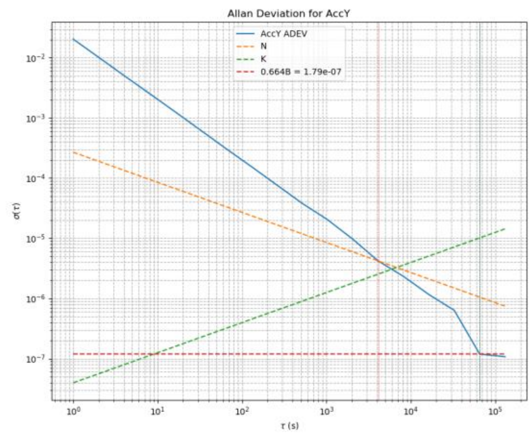
Allan Deviation for AccY
AccY ADEV
N
K
0.664B = 1.79e-07
σ(τ)
τ (s)

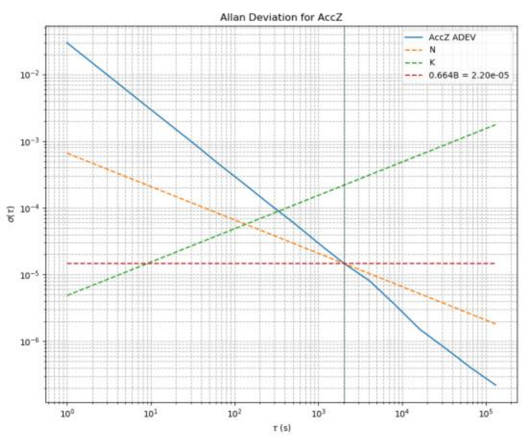
Allan Deviation for AccZ
AccZ ADEV
N
K
0.664B = 2.20e-05
σ(τ)
τ (s)

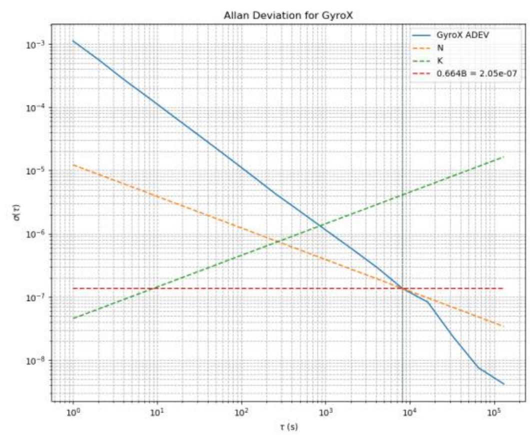
Allan Deviation for GyroX
GyroX ADEV
N
K
0.664B = 2.05e-07
σ(τ)
τ (s)

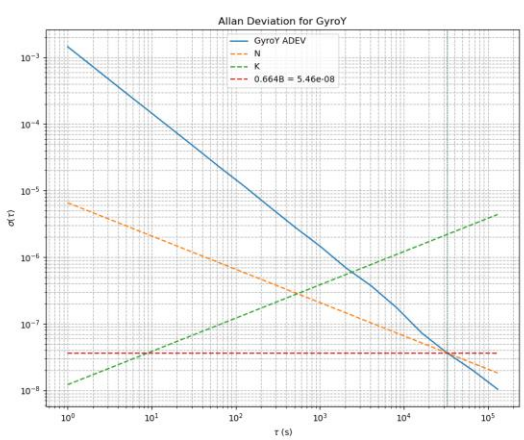
Allan Deviation for GyroY
GyroY ADEV
N
K
0.664B = 5.46e-08
σ(τ)
τ (s)

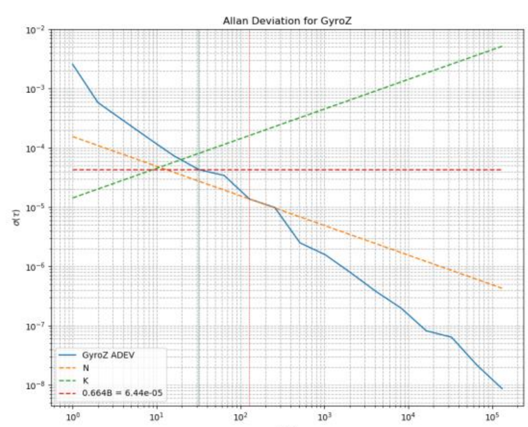
Allan Deviation for GyroZ
GyroZ ADEV
N
K
0.664B = 6.44e-05
σ(τ)
τ (s)

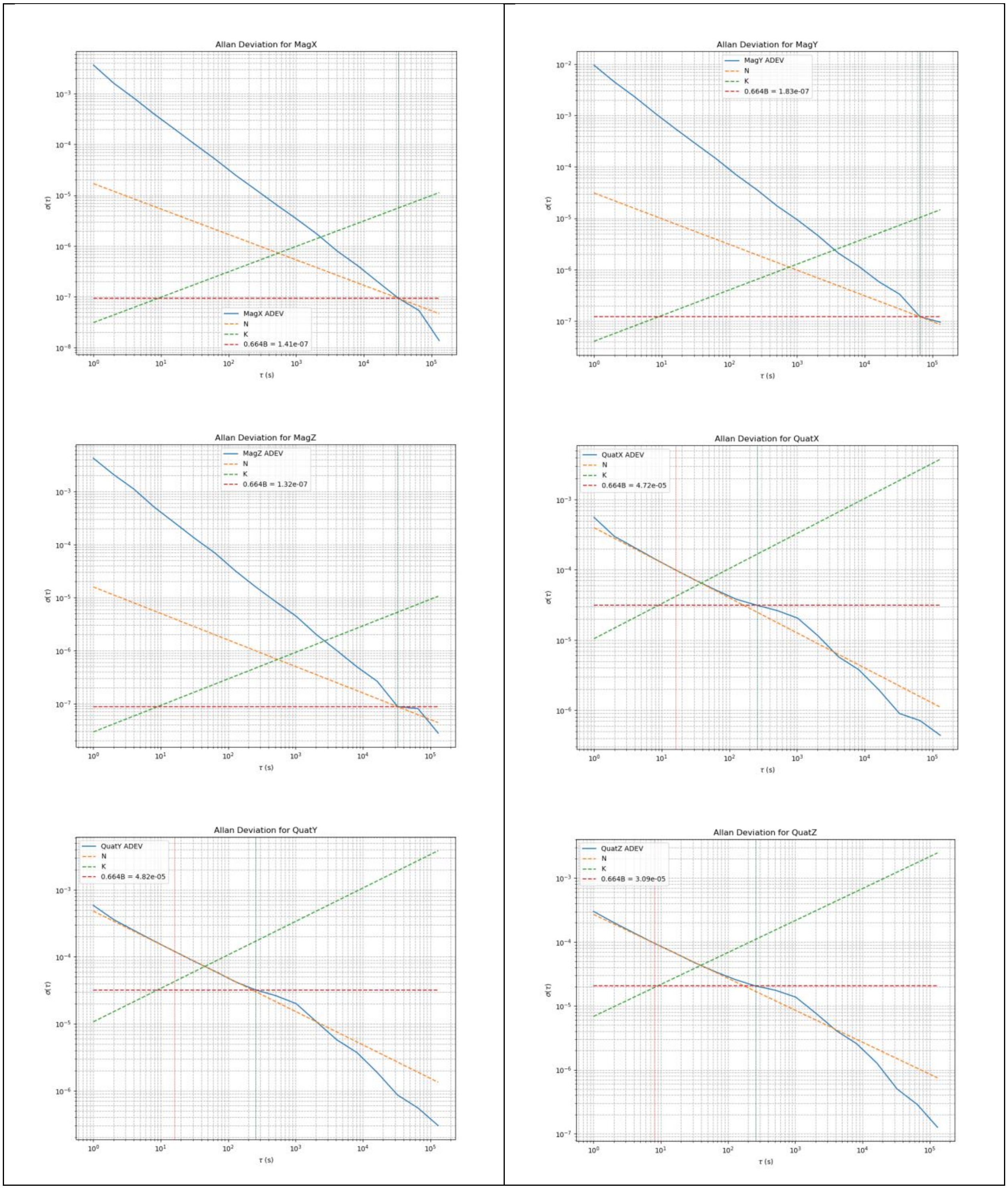

Analysis:

Using the Allan Variance plots for angular velocity and linear acceleration across three axes, we gained insights into our system's inherent noise characteristics, such as White Noise, Rate

Random Walk, and Bias Instability. The consistency between our graphs and the typical Allan Variance signature indicates minimal external disturbances during our measurements.

From the plot contours, the pronounced downward slope at the beginning signifies White Noise. This type of noise is dominant at short integration times, and its effects diminish as the square root of the integration time increases. The curve's plateauing, especially where there's a discernible trough or "valley", points to Bias Instability. Although a distinct "valley" is not immediately apparent in our plots, the leveling off suggests the possible presence of bias instability or a random walk. This region typically marks the sensor's optimal noise performance for the given integration times. On the other hand, Rate Random Walk or Drift would manifest as a rising slope on the Allan Deviation plot. In our data, no such slope is prominent, indicating an absence of rate random walk or drift for the integration times in focus.

Beyond these findings, there are other potential error contributors in inertial sensors that might not be directly evident from the Allan Deviation plots. These include variations in the sensor bias due to temperature changes, mismatches between the anticipated and actual sensor readings for a given input, and the skewing of sensor axes which can introduce errors. In essence, the predominant noise types in our plots are white noise and a potential bias instability or random walk, with no overt sign of rate random walk or drift within the observed integration times.

Identifying the White Noise or Angle Random Walk coefficients (N) was rather straightforward. On the Allan Variance graph, the descending slope at half angle was our marker. By fitting a line to this segment and noting its value when tau was one, we successfully determined N.

Determining the Rate Random Walk coefficient (K) was a tad more complex. The typical approach is to look for a section of the graph with an ascending slope at half an angle, fit a line, and then check its value at tau equals three. A slight rightward curve was observed in our plots. Although this curve had minimal effects on the data for GyroX, GyroY, AccX, and AccZ, it impacted the results for GyroZ and AccY. Nevertheless, the derived K values were consistent with the rest.

The Bias Instability coefficient (B) involved tracing a horizontal line near the graph's lowest point. Almost all our plots were compliant, with GyroX being a slight exception. Yet, the deviation was minimal and consistent with our overall data.

For benchmarking, we consulted the VN-100 manual. For the accelerometer, it listed a bias stability of 0.04 mg (equivalent to $3.924 * 10^{-4}$ m/s^2) and a noise density value of 0.14 m/√Hz (or $1.3734 * 10^{-3}$ $m/\sqrt{s^2 * Hz}$). For the gyroscope, the bias stability was 10 °/hr (or $4.8481 * 10^{-5}$ °/s), and the noise density was 0.0035 °/√Hz (approximately $6.1087 * 10^{-4}$ °/s/√Hz).

Our B values closely aligned with the VN-100's bias stability, and our N values were consistent with its noise density figures. Ideally, our measurements would align even more closely with the

VN-100's specifications. However, external factors, like individuals moving around in our testing environment at NEU, could have slightly skewed our results.